Chinese Journal of
POLYMER SCIENCE

RESEARCH ARTICLE

https://doi.org/10.1007/s10118-026-3878-0
Chinese J. Polym. Sci.

Cracking Behavior Analysis of Thermoplastic Polyimide under Vacuum Pressure Impregnation

Chao Xiao, Xian Zhang, Long-Gui Zheng*, Ye-Zheng Xiao, and Yan-Lan Hu

Hefei Institutes of Physical Science, Chinese Academy of Sciences, Hefei 230031, China

Electronic Supplementary Information

Abstract Thermoplastic polyimide (TPI) insulated wires, which exhibit excellent insulating and radiation-resistant properties at extremely low temperatures, are designated as connection lines for the quench detection system of superconducting magnets. However, extensive cracking was unexpectedly observed after the implementation of vacuum pressure impregnation (VPI). The cracking behavior of TPI-insulated wires during the VPI process was systematically investigated. The results reveal that the failure is a multi-factor coupled phenomenon involving synergistic interactions between thermal, mechanical, and chemical mechanisms. First, the coiled configuration imposes sustained tensile stress on the outer arc of the insulation, while the extrusion process introduces molecular orientation and residual stresses into the TPI matrix. Although the VPI temperature (130 °C, 72 h) is well below the glass transition temperature (about 245 °C), sub-T_g segmental relaxation and amorphous structural rearrangement occurred, leading to free volume redistribution and residual stress relaxation. The constraint of the metallic conductor further restricts dimensional recovery, thereby promoting microcrack initiation. Second, low-molecular-weight species from the epoxy system, particularly the curing agent HY918 and the accelerator DY073-1, permeate into the amorphous regions of TPI, causing plasticization, swelling, and enhanced segmental mobility, which significantly reduces the local resistance to yielding and crack propagation. Under sustained bending stress, this results in a typical environmental stress cracking (ESC) acceleration effect. Third, the substantial mismatch in the coefficients of thermal expansion between the TPI and the metallic conductor generates considerable thermal stresses during the VPI thermal cycle, further exacerbating the cracking risk. Based on the mechanistic understanding, a protective strategy was implemented by wrapping the TPI wires with a thermal insulation layer prior to VPI. The protected specimens successfully passed the vacuum Paschen test, confirming that this approach effectively prevented resin permeation and thermally induced structural transitions in TPI insulation. This strategy provides a reference for the failures of quench diagnostic wires in similar superconducting magnets.

Keywords Thermoplastic polyimide; Segmental relaxation; Environmental stress cracking; Electrical insulation

Citation: Xiao, C.; Zhang, X.; Zheng, L. G.; Xiao, Y. Z.; Hu, Y. L. Cracking behavior analysis of thermoplastic polyimide under vacuum pressure impregnation. *Chinese J. Polym. Sci.* https://doi.org/10.1007/s10118-026-3878-0

INTRODUCTION

Aromatic and imide groups within the monomer units confer rigidity and robust interchain interactions on the polyimides, which in turn yield exceptional thermal stability and superior mechanical properties.[1,2] Owing to their ability to withstand the harsh operating environment of superconducting magnet devices, high-performance thermoplastic polyimide (TPI) insulated wires are typically employed as voltage tap connections for quench detection systems.[3,4] Therefore, the reliability and performance of the magnet system are largely dependent on the mechanical robustness of these wires.[5] To further enhance the insulation performance of magnets, vacuum pressure impregnation (VPI) treatment is mandatory per design specifications to encapsulate the magnets and diagnostic wires into an integrated assembly. VPI treatment refers to a process that removes air and moisture from the interior of coils *via* vacuum pumping, impregnates the epoxy resin system into the gaps of the coils under pressure, and forms a dense insulating structure after heating and curing.[6] However, obvious cracking occurred on some TPI wires after VPI treatment during laboratory-scale specimen preparation. Specifically, many cracks perpendicular to the length direction appeared at the bent parts of the wires, and some cracks penetrated the insulation layer, resulting in wire exposure. This seriously impairs the reliability of the quench diagnosis system and overall insulation performance of the laboratory sample.

In the traditional magnet manufacturing process, the magnet is first subjected to VPI treatment followed by the connection of TPI diagnostic wires; thus, no cracking of the TPI has been observed. However, the joints formed by this operation become the weak points in the entire diagnostic system. To improve the reliability of the diagnostic system, researchers

* Corresponding author, E-mail: zlonggui@ipp.ac.cn
Received June 9, 2026; Accepted September 7, 2026; Published online November 2, 2026

© Chinese Chemical Society
Institute of Chemistry, Chinese Academy of Sciences

have attempted to connect the TPI wires to the magnet first before performing the VPI impregnation treatment on them together. At present, the cracking mechanism of the TPI insulation layer under the special process of VPI process has not been reported, and targeted solutions have not been proposed. Corrosion by chemical reagents is considered to be a potential influencing factor. Piccin *et al.*[7] proposed that TPI may undergo accelerated brittle failure under the combined action of amine curing agents, mechanical stress, and heating conditions, and classified this phenomenon as environmental stress cracking (ESC). Goodwin *et al.*[8] investigated the response of TPI immersed in different solvents, revealing that specific solvents cause reduced the glass transition temperature (T_g) and ESC *via* surface energy reduction and matrix plasticization. Solvent-induced secondary crystallization was also observed. However, anhydride-based curing agents were used in the VPI process in this study. Notably, TPI was susceptible to cracking, even in the absence of epoxy resin contact. However, systematic and comprehensive solutions have not yet been proposed.

To address this critical issue, this study is the first to systematically uncover the cracking mechanism of TPI wires during the VPI process for the first time. Through a multi-dimensional coupled analysis of material intrinsic properties and environmental factors, it accurately verifies the cracking causes and proposes a simple yet effective solution. This work fills the research gap in the failure mechanism of TPI materials in the core insulation process of superconducting magnets and provides a systematic methodology for compatibility research between polymer insulation materials and impregnation processes.

DESIGN AND IMPLEMENTATION

Experimental Materials

The original TPI wires (denoted as TPI-1) were featured an AWG 20 gauge with an overall diameter of 2.8–3 mm, and conductor diameter of 1.009 mm. Its insulation layer was composed of a continuously extruded TPI AURUM™, with a rated voltage of 30 kV. Cracked TPI wires, designated as TPI-2, were cut from the coil that had undergone the VPI process. The epoxy resin and curing agent used in the VPI process were sourced from Huntsman, comprising GY282 (a bisphenol F-type low-viscosity epoxy) as the base resin, HY918 (anhydride curing agent) as the main curing agent, and DY073-1 (a compound of tributylamine, phenol, and diethyl phthalate) as the accelerator. The thermal insulation film (thickness: 0.3 mm, thermal conductivity: 0.035 W/(m·K)) were procured from Anhui Zhongke Yushun Technology Co., Ltd.

Experimental Process

The VPI treatment process is briefly described as follows. The stainless steel armored prototypes with soldered TPI wires were placed in a sealed mold, which was then evacuated to a vacuum level of 100 Pa, followed by the injection of a mixture of epoxy resin and curing agent. The mold was heated to 130 °C at a heating rate of 5 °C/h and held at this temperature for 72 h. Finally, the mold was cooled down to room temperature, and the prototypes were demolded. The excess length of the extended TPI wire was coiled into loops and sealed with silicone rubber for protection. The exposed straight line area is protected using a heat-shrinkable sleeve. The detailed structure of the sample is shown in Fig. 1(a).

Corrosion test of epoxy resin system on linear wires. Two

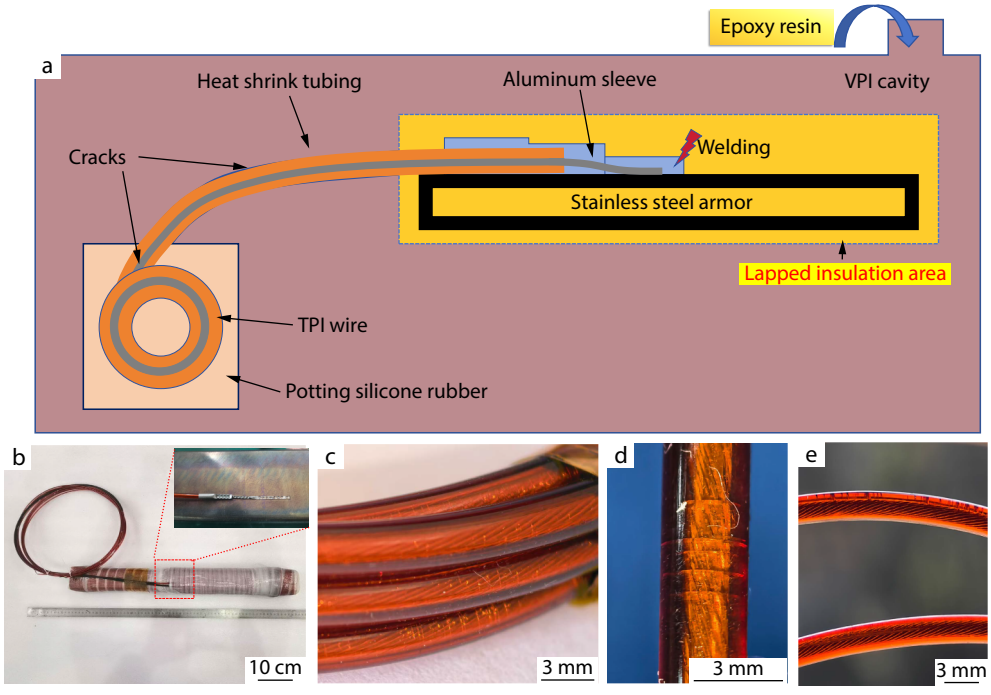


Fig. 1 (a) Schematic diagram of the prototype undergoing VPI treatment; (b) Photograph of the prototype where the TPI diagnostic wire passes through the stainless steel armor, the inset in the upper right corner shows the welding joint between the diagnostic wire and the armor; the entire armor was insulated and sealed by helical wrapping with epoxy resin/glass fiber cloth/polyimide film; (c–e) Photographs of insulation layer cracking on the TPI wire.

https://doi.org/10.1007/s10118-026-3878-0

pieces of original TPI wires approximately 40 cm in length were cut off. One was manually bent with a bending radius of approximately 0.5 cm and a bending angle of more than 100°. The surface of the other wire was coated with a mixture of epoxy resin and curing agent, then placed in an oven and treated at 130 °C for 72 h. After curing, it was manually bent using the same parameters. The results are shown in Fig. 2.

Corrosion test of the epoxy resin system on circular coils. A piece of original TPI wire with a length of approximately 100 cm was cut off and formed into a circular coil with a bending radius of 3 cm. Half of the coil was covered with adhesive tape, and the other half was coated with a mixture of epoxy resin and curing agent. The samples were then placed in an oven and treated at 130 °C for 72 h. The results are shown in Fig. 3.

Corrosion test of single component of epoxy resin on circular coils. Three identical circular coils were separately coated on their surfaces with epoxy resin GY282, the curing agent HY918, and accelerator DY073-1, respectively. The coated coils were then maintained at ambient temperature for three days, and the outcomes are illustrated in the accompanying Fig. 4.

Preparation of TPI thin film: TPI insulation layer was peeled off from the original wires, then hot-pressed into sheet samples with thickness of approximately 0.2 mm at 380 °C under a pressure of 1 MPa for 5 min, also denoted as TPI-1.

TPI film heat treatment: the TPI-1 film was placed in an oven and baked at 130 °C for 3 days, marked as TPI-1-130°C@3d.

TPI film coating treatment: one side of the TPI-1 film (A) was separately coated with HY918 and DY-073-1, while the opposite side was left uncoated. The resulting samples were

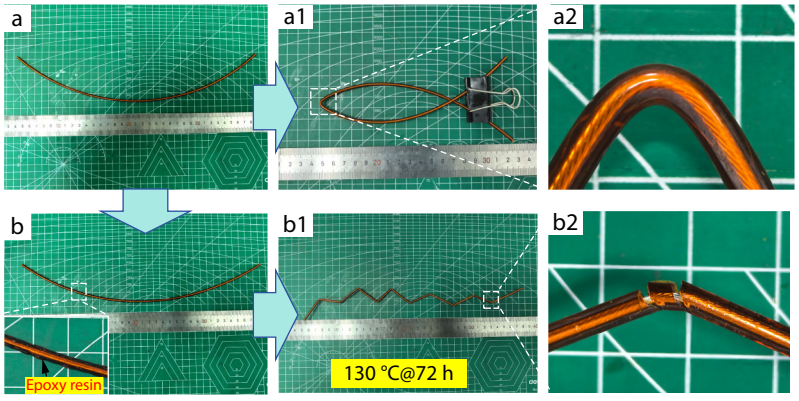


Fig. 2 Effect of epoxy resin on straight-type TPI wires. (a) Straight-type TPI-1 wire; (a1) Photograph of the straight-type TPI-1 wire subjected to a large-angle bend; (a2) Magnified view of the bent part in (a1); (b) Straight-type TPI-1 wire with epoxy resin mixture coated on its surface; (b1) Bending photograph of the sample in (b) after baking at 130 °C for 72 h; (b2) Magnified view of the bent part in (b1).

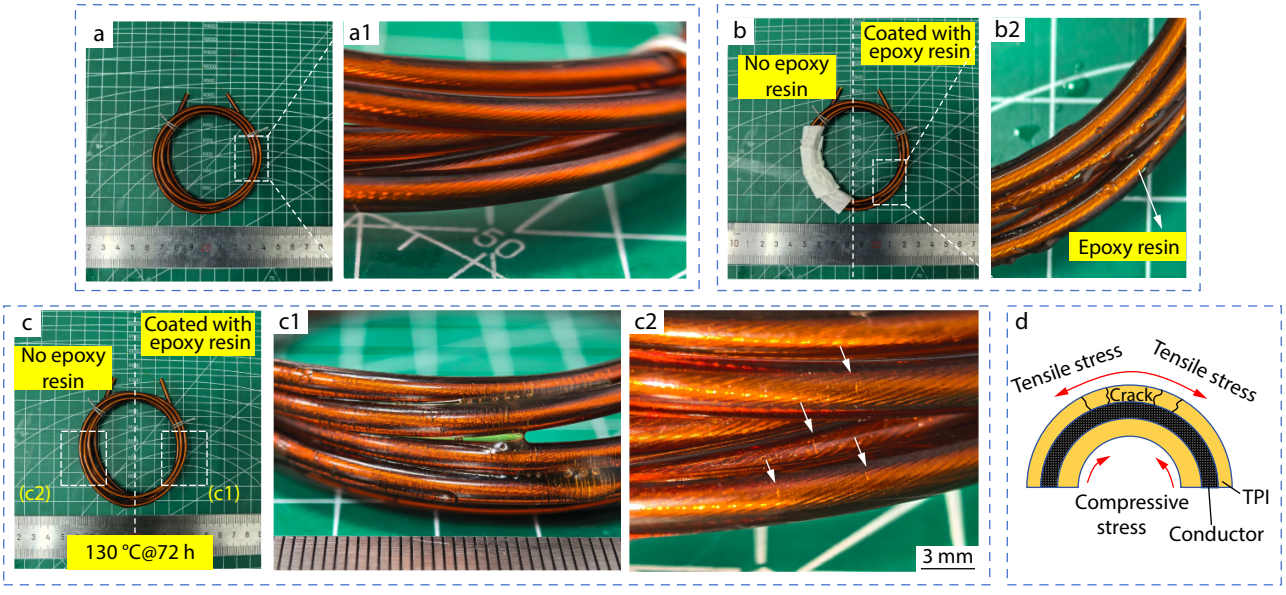


Fig. 3 Effect of epoxy resin on circular TPI wires. (a) Original TPI-1 wire coil with a bending radius of 3 cm; (a1) Partial magnified view of (a); (b) The TPI-1 coil in (a) with half of its surface coated with epoxy resin mixture (right side) and the other half wrapped with adhesive tape to avoid contact with epoxy resin mixture (left side); (b1) Partial magnified view of the epoxy resin-coated area in (b); (c) Photograph of the sample in (b) after baking at 130 °C for 72 h; (c1) Partial magnified view of the epoxy resin-coated area in (c); (c2) Partial magnified view of the uncoated area in (c); (d) Schematic diagram of the bending stress on the wire.

https://doi.org/10.1007/s10118-026-3878-0

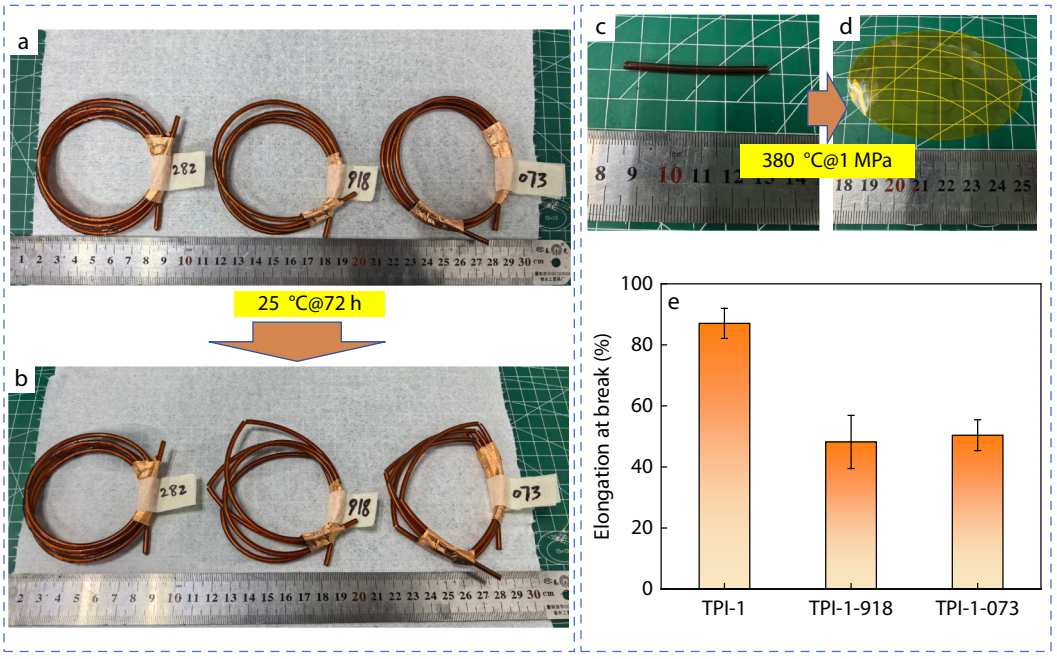


Fig. 4 Influence of epoxy resin and curing agents on circular TPI-1 wires. (a) TPI coils coated with epoxy resin and curing agents; (b) Coils in (a) after placed at 25 °C for 72 h; (c) Raw TPI-1 insulation layer (conductor removed); (d) TPI-1 film from hot-pressing of (c) insulation layer; (e) Elongation at break of TPI-1 coated with different curing agents (25 °C for 72 h).

designated TPI-1-918 and TPI-1-073, corresponding to the two coating agents.

Thermal insulation protection test: a piece of the original TPI wire with a length of approximately 100 cm was used, and its surface was helically wrapped with a thermal insulation film at an overlapping rate of 50%. The wire was then formed into a circular coil with a bending radius of 3 cm, and the surface of the sample was coated with epoxy resin. Subsequently, the samples were placed in an oven and heated at 130 °C for 72 h.

Characterizations

A thermogravimetric analyzer (TGA 209, TA Instruments, USA) was used to characterize the thermal stability of TPI. The samples were heated from room temperature to 700 °C at a heating rate of 10 °C/min under a nitrogen atmosphere, and the curves of sample weight change with temperature were recorded. To investigate the changes in the crystal structure of the TPI material, approximately 10 mg of the TPI sample was tested using a differential scanning calorimeter (NETZSCH, DSC-214). Under a high-purity nitrogen atmosphere for protection, the sample was heated from room temperature (25 °C) to 450 °C at a heating rate of 10 °C/min, held at this temperature for 2 min, and then cooled down to 50 °C at a cooling rate of 10 °C/min. By analyzing the heating and cooling curves, parameters such as the glass transition temperature (T_g), cold crystallization temperature (T_c), crystallization enthalpy (ΔH_c), melting temperature (T_m), and melting enthalpy (ΔH_m) of the sample were obtained. A thermomechanical analyzer (TMA, Q400, TA Instruments) was used to characterize the coefficient of thermal expansion (CTE) of the TPI material. Two measurement modes were used. In the tensile mode, the film specimens were cut into rectangular splines with a width of 4.7 mm and a length of 7.37 mm. A constant tensile stress of 0.2 N was applied during the test, and the specimens were heated from room temperature to 200 °C at a ramp rate of 5 °C/min, with the corresponding length change continuously recorded. In the compression mode, TPI insulation tubes with polished flat ends were used, with a specimen height of 2.47 mm. The compression tests were conducted under a constant compressive load, following the same heating protocol, and the dimensional changes along the axial direction were monitored. For both modes, the coefficient of thermal expansion (CTE) over the measured temperature range was calculated as the relative change in specimen dimension per unit temperature change, *i.e.*, CTE = $\Delta L/(L_0 \cdot \Delta T)$, where ΔL is the dimensional change, L_0 is the original gauge length (or initial height), and ΔT is the temperature interval. Fourier transform infrared (FTIR) spectroscopy (Spectrum Two, PerkinElmer, UK) was utilized to identify the characteristic functional groups of the TPI film, the curing agent (HY918), and the accelerator (DY073-1). The measurements were performed in attenuated total reflectance (ATR) mode using a diamond ATR accessory. All spectra were recorded at ambient temperature in the wavenumber range of 4000–400 cm^{-1}. X-ray diffraction (XRD) measurements were performed on a Rigaku Smartlab 9 kW diffractometer employing Cu-Kα radiation (λ=1.54051 Å). The diffraction patterns were acquired in the step-scan configuration over a 2θ interval of 5°–80° at a constant scan rate of 20 (°)/min. The tensile properties of dumbbell-shaped specimens were tested for tensile properties on a YY-5000 universal testing machine (Yangzhou Tianyou Instrument Equipment Co., Ltd., China) at a crosshead speed of 25 mm/min. The specimens were prepared in a dumbbell shape (Fig. S2 in the electronic supplementary information, ESI), and three replicates were tested for each sample to obtain average values. The specimens were then subjected to different treatment methods. The original specimen was designated as TPI-1; the specimens with their surfaces coated with curing

agent were labeled TPI-1-918 and TPI-1-073, respectively; the specimen undergoing heat treatment at 130 °C for 72 h was coded as TPI-1-130°C@3d. A Megger MIT1525 insulation resistance tester was used for the vacuum Paschen test. First, the samples treated with VPI were connected to the positive electrode of the power supply and then placed into a vacuum chamber. After sealing the chamber, a vacuum pump was activated to evacuate it to the set vacuum level. Subsequently, the high-voltage power supply is switched on. The voltage was increased gradually, and whether the discharge or breakdown phenomena occurred on the surface of the device was observed. The critical breakdown voltage and discharge resistance were recorded.

RESULTS AND DISCUSSION

Analysis of the Cracking Phenomenon of the TPI Wires

The TPI diagnostic wire and stainless steel armor were welded using an aluminum sleeve. The entire stainless steel armor and joint were insulated and wrapped with multiple layers of epoxy resin/glass fiber cloth/polyimide film, followed by curing to form a seal.[9,10] The straight part of the extended wire was protected by heat-shrink tubing to avoid contact with the epoxy resin. The excess length of the TPI wire was coiled into a loop and sealed with silicone rubber. The entire prototype was placed in a vacuum chamber for epoxy resin casting, as shown in Fig. 1(a). The prototype before VPI treatment is shown in Fig. 1(b). After the VPI treatment, cracking was observed on the surface of the TPI wires. The cracks were distributed both in the straight section of the wire (Fig. 1d) and in the bent parts of the coil (Fig. 1c). Although the surfaces of the TPI wires in the exposed sections were protected to prevent contact with the VPI epoxy resin, cracking still occurred after VPI treatment.

As can be seen from the Figs. 1(c)–1(e), the cracks were mainly distributed on the outer side of the bent parts of the wires, while no cracks were found on the inner side. A few cracks were observed in the straight sections. The cracks at the fractured locations were perpendicular to the length direction of the wires, and individual cracks have propagated to the conductor region, resulting in exposure of the wire conductors. Thus, it can be inferred that the internal-external stress difference caused by bending is one of the factors inducing cracking. According to the experience of the International Thermonuclear Experimental Reactor (ITER), TPI wires exposed to high-concentration amine curing agents and under constant strain were confirmed to suffer from ESC. Degradation starts during manufacturing. Many crazes were formed on the tensile-stressed wire bodies prior to the total fracture. Although the curing agent used in this work was acid anhydride, the corrosive behavior of the epoxy resin was also verified.

Effect of Epoxy Resin Mixture on TPI

Previous studies have demonstrated that TPI is vulnerable to penetration and degradation effects induced by small molecule species.[11] Although, the exposed segments of the TPI wires in this work were meticulously shielded from direct epoxy contact during processing, the possibility of epoxy ingress cannot be entirely excluded. Under high-vacuum conditions, the low-viscosity epoxy formulation may permeate through the welded aluminum tube joints and subsequently migrate into the TPI wire along the conductor. This potential migration pathway is further promoted by the stranded structure of the conductor, which comprises multiple twisted fine wires and contains continuous internal voids that act as wicking channels. A comparative verification test was conducted to confirm the corrosion effect of the epoxy resin system. The original TPI wire showed a naturally bent state when unwound from the reel, as shown in Fig. 2(a), with a bending radius of nearly 50 cm, which is defined as a straight-type wire. Even when the wire was bent at a radius of 0.5 cm with an angle of more than 100°, the TPI insulation layer remained intact, as shown in Fig. 2(a2). For comparison, epoxy resin was coated on the surface of the TPI-1 wire and subjected to a curing process at 130 °C for 72 h. However, a slight bending by a manual external force can cause TPI cracking. The wires coated with epoxy resin could be manually shaped into a Z-shape, with obvious cracking occurring at the bent parts (Figs. 2b1 and 2b2). This result confirms that the epoxy resin system in this study exerts an embrittlement effect on the TPI. Through disassembly of the samples, it was confirmed that the epoxy resin could penetrate approximately 2 m in length from the welded joint into the TPI wire interior. Therefore, it can be concluded that cracking within this length range is predominantly caused by epoxy resin attack.

To verify that the embrittled TPI no longer possessed sufficient mechanical strength to withstand the differential tension between the inner and outer layers of the circular coil, thereby leading to cracking, a mixture of the epoxy resin systems was applied to the surface of the circular coils. The coils were prepared at the minimum bending radius specified by the wire manufacturer (3 cm) to maximize the local tensile strain on the insulation and thereby amplify any degradation effects induced by the respective coating agents.

As illustrated in Fig. 3(a), a 1-meter-long TPI-1 wire was coiled into a circular coil with a diameter of 6 cm. For the test setup, the right half of the coil was coated with an epoxy resin mixture, whereas, the left half was wrapped with adhesive tape to prevent contact with the epoxy resin, serving as a blank control group. After undergoing high-temperature curing at 130 °C for 72 h, the test results are presented in Figs. 3(c1) and 3(c2), respectively. As shown in Fig. 3(c1), extensive cracking occurred in the epoxy resin-coated area. This further confirms that the embrittlement effect of the epoxy resin significantly reduces the mechanical strength of the TPI insulation layer, whereas the tensile stress on the outer side of the bent wire further accelerates crack propagation (Fig. 3d).

To further identify which specific component of the epoxy resin system is responsible for the embrittlement of TPI, three individual constituents—the epoxy resin, the main curing agent, and the accelerator—were separately applied onto the surface of the TPI coils. After being left at room temperature for three days, it was found that the two coils coated with the main curing agent and the accelerator both exhibited obvious cracking, while the coil coated with the epoxy resin monomer remained intact in a circular shape (Fig. 4b). These results demonstrate that anhydride, and amine/phenol-complex-based small molecules exhibit a higher propensity to permeate TPI and thereby induce ESC.

https://doi.org/10.1007/s10118-026-3878-0

This result is related to the plasticization effect of the curing agents. During the curing process of the epoxy resin, small molecules such as free anhydrides or modified amine complex accelerator derivatives in the system slowly diffuse to the TPI interface. These small molecules can penetrate into the gaps between the TPI molecular chains, weakening the intermolecular forces through swelling and polar interactions. Thus, segmental mobility was enhanced, and the tensile strength of the TPI decreased accordingly.[8] This conclusion can be drawn from Fig. 4(e) where the elongation at break of the TPI specimens coated with the two curing agents exhibits a significant deterioration. Consequently, when subjected to bending forces, the damaged molecular chains cannot effectively disperse stress. Instead, stress concentrates at the structural defects, which initiate microcracks. These microcracks then propagate rapidly, ultimately making polyimide prone to cracking during bending. Generally, the intensity of such plasticization effects is closely linked to the temperature. Higher temperatures amplify the plasticization effect, leading to greater damage to the insulation layer.

Notably, Fig. 3(c2) reveals that a small number of cracks still emerged on the left uncoated side after high-temperature baking, despite no direct contact with the epoxy resin. This phenomenon is consistent with the cracking observed in earlier prototypes (Fig. 1a). This finding suggests that the plasticization behavior of curing agents under bending stress is not the sole factor that induces TPI cracking. However, the heat treatment process alone may also exert a negative impact on the structural integrity of the TPI material.

ATR-FTIR spectroscopy was employed to provide microscopic evidence of the permeation of the small molecules. As shown in Fig. 5(a), the bands at 1844 and 1771 cm^{-1} correspond to the asymmetric and symmetric stretching vibrations, respectively, of the anhydride carbonyl groups in the HY918 curing agent, while the multiple bands in the range of 1242–1168 cm^{-1} are attributed to the asymmetric C—O—C stretching vibration of the anhydride moiety. For the accelerator DY073-1, the characteristic bands are mainly observed at 1722 and 1280 cm^{-1}, which are assigned to the ester carbonyl (C=O) and C—O stretching vibrations of diethyl phthalate, respectively; the signals corresponding to tributylamine and phenol are relatively weak. The pristine AURUM TPI-1 film exhibits characteristic absorption bands at 1777 and 1716 cm^{-1}, assignable to the asymmetric and symmetric stretching vibrations of the imide ring C=O, respectively. The band at 1590 cm^{-1} corresponds to the aromatic ring C=C skeletal stretching vibration, the band at 1360 cm^{-1} is attributed to the imide ring C—N stretching vibration, and the band at 1224 cm^{-1} is associated with the asymmetric stretching of the aromatic ether linkage.[12,13] A comparison revealed that there

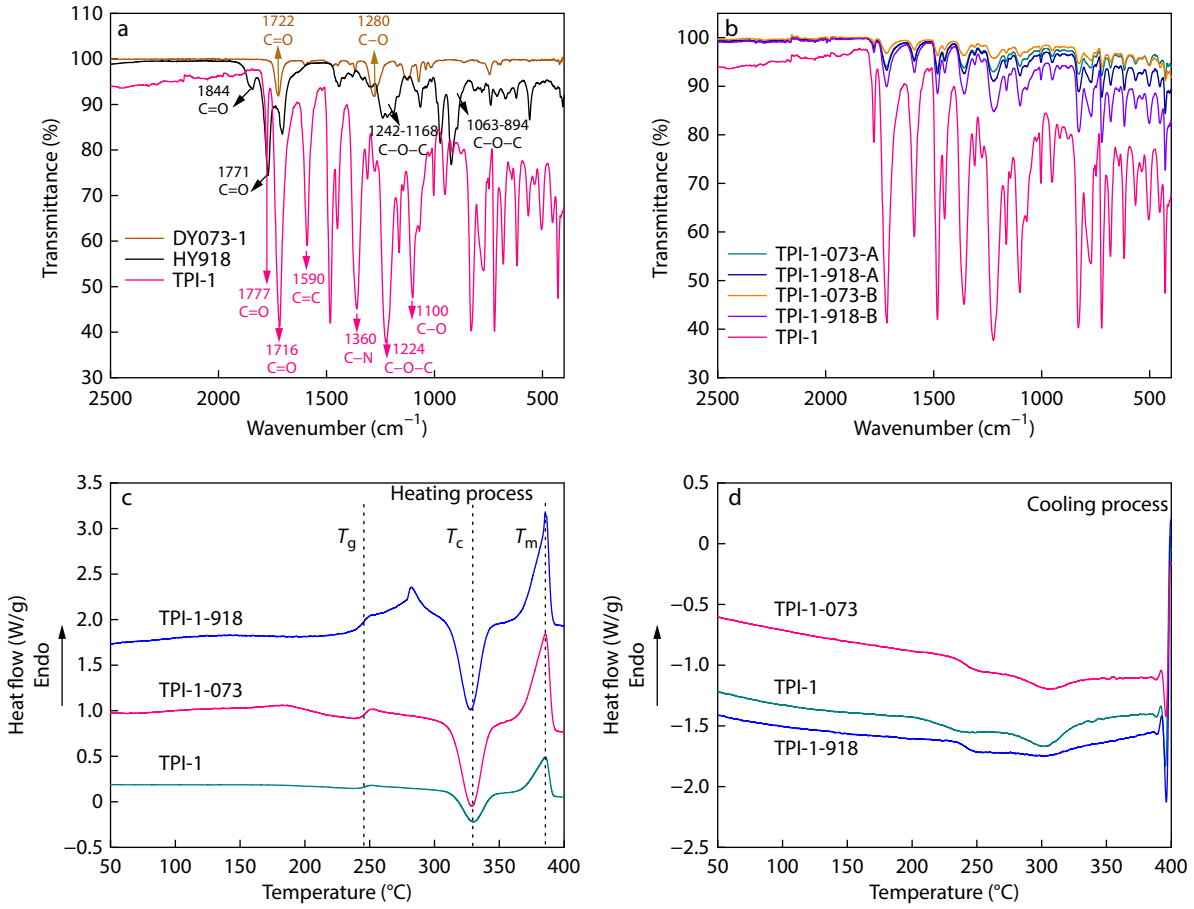


Fig. 5 (a) ATR-FTIR spectra of HY918, DY073-1, and pristine TPI-1; (b) ATR-FTIR spectra of the coated (A-side) and uncoated (B-side) surfaces of TPI-1 films after separate application of HY918 and DY073-1; (c) DSC heating curves and (d) cooling curves of TPI samples coated with the curing agent and the accelerator.

https://doi.org/10.1007/s10118-026-3878-0

is a considerable degree of spectral overlap between the characteristic peaks of the curing agent/accelerator and those of TPI-1. Fig. 5(b) presents the ATR-FTIR spectra of both the A-side (coated) and B-side (uncoated) surfaces of the TPI-1 films after the separate application of HY918 and DY073-1. In all cases, no new characteristic peaks corresponding to the curing agent or accelerator were detected, and the spectra exclusively exhibited intrinsic features of TPI. This observation can be attributed to two possible reasons. First, the substantial spectral overlap may result in weak signals of the penetrant molecules being masked by the intense intrinsic absorption of the TPI matrix. Second, the small molecular additives may have gradually diffused into the interior of the TPI film over the three-day standing period, leading to a reduced concentration at the surface that fell below the detection limit of the ATR mode, which typically probes only the top hundreds of nanometers to approximately 1 μm in depth. The plasticizing effect of the small molecules was more prominent in the DSC results. As depicted in Fig. 5(c), the publicly reported thermal transitions of the neat AURUM TPI are approximately 245 °C for T_g, 388 °C for T_m, and 330 °C for the cold crystallization temperature (T_c).[14] After coating with HY918, the sample exhibited a distinct endothermic peak at approximately 280 °C. For the DY073-1-coated sample, a chain segment relaxation endotherm appeared below T_g (at approximately 200 °C). These thermal anomalies collectively confirm that the ingress of small molecules into the amorphous regions of TPI promotes localized chain segment mobility, alters the free volume and intermolecular interactions, and consequently, reduces the local fracture resistance.[15] The DSC cooling curves is shown in Fig. 5(d). It can be observed that the curing agent and accelerator cause the T_g of TPI to shift slightly away from that of TPI-1, further demonstrating that small molecules can alter the local segmental relaxation dynamics at the TPI surface.

Effect of Heat Treatment on TPI

As shown in Fig. 3(c2), thermal treatment alone may influence the TPI structure, even though the treatment temperature is far below the glass transition temperature (T_g). A series of analyses were conducted to elucidate this anomalous phenomenon.

First, the potential effects of thermo-oxidative ageing were examined. Fig. 6(a) shows the thermogravimetric curves of the insulation layers of the TPI-1 and TPI-2 under nitrogen atmosphere. Typically, the temperature corresponding to 5% mass loss is defined as the initial decomposition temperature.[16] Based on this criterion, the thermal decomposition temperatures of both the original and cracked TPI wires exceeded 500 °C. Moreover, the FTIR spectra of the TPI-1 before and after thermal treatment were completely superimposable, confirming that TPI exhibited excellent thermo-oxidative stability and did not undergo decomposition at 130 °C.

Second, DSC was employed to investigate the thermal properties of the TPI. It was found that the cracked wire (TPI-2) exhibited T_g and T_m values identical to those of TPI-1; however, the cold crystallization temperature (T_c) decreased by 8.69 °C. After thermal treatment at 130 °C for 3 days, the T_c of TPI further decreased by 26.73 °C. This substantial difference is also evident in the DSC cooling curves. As shown in Fig. 6(d), the thermal treatment led to an increase in the cooling crystallization temperature of TPI. These results indicate that thermal exposure altered the microstructure/thermal history of amorphous TPI, thereby enhancing its crystallization capability during subsequent heating and cooling cycles.

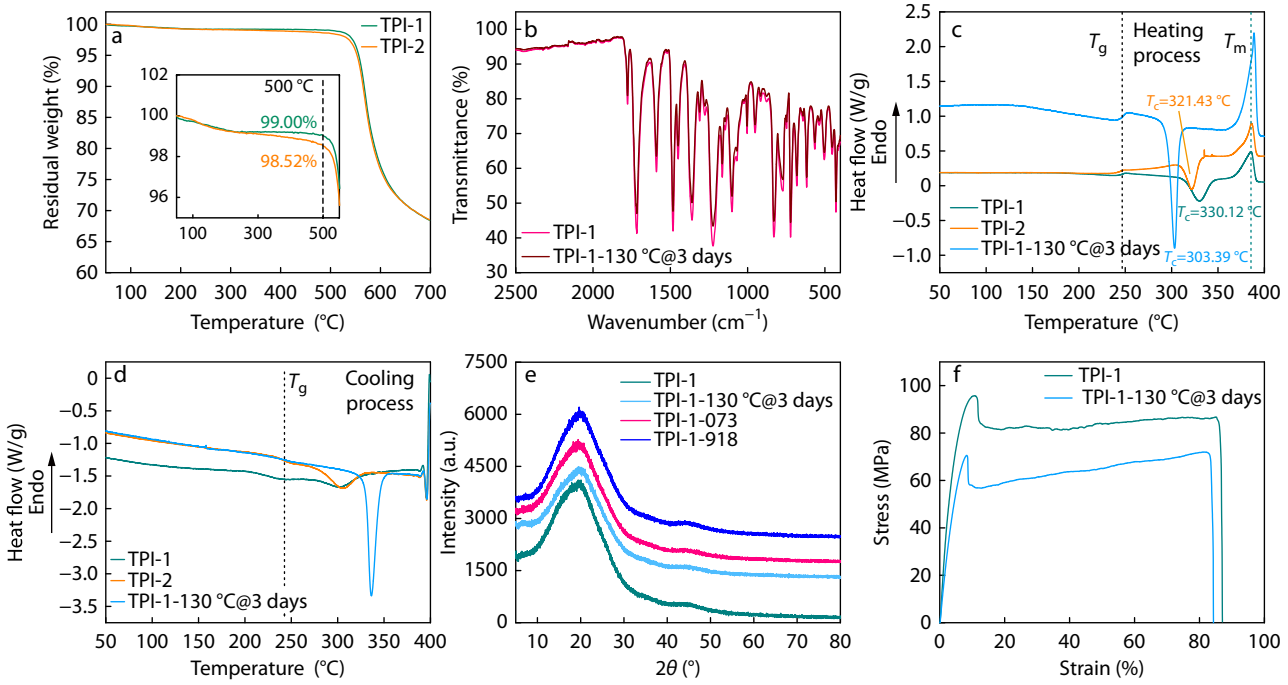


Fig. 6 (a) Thermogravimetric (TG) curves of the pristine TPI-1 and cracked TPI-2 wires; (b) ATR-FTIR spectra of the TPI-1 film before and after thermal treatment at 130 °C for 3 days; (c) DSC heating curves; (d) DSC cooling curves; (e) XRD patterns of TPI-1 under various treatment conditions; (f) Stress-strain curves of the TPI-1 film before and after thermal treatment at 130 °C for 3 days.

https://doi.org/10.1007/s10118-026-3878-0

AURUM-TPI is a thermoplastic polyimide that inherently possesses crystallization potential but exhibits very slow crystallization kinetics. Fig. 6(e) shows that TPI-1 remained amorphous under all treatment conditions, with no detectable cold crystallization at 130 °C. Nevertheless, amorphous segments may also undergo a certain degree of local rearrangement. Its T_g primarily corresponds to α-relaxation, which involves large scale cooperative segmental motion of the polymer main chains. Secondary β/γ relaxations arising from non-cooperative local motions of aromatic rings, ether linkages, and chain segments are known to occur well below T_g.[17] Sub-T_g β/γ relaxations in aromatic thermoplastic polyimides have also been well documented in the literature.[18]

In addition, the extruded wire is not an ideal, stress-free free-standing film. During the extrusion process, the TPI undergoes rapid cooling that freezes in the molecular orientation, while simultaneously developing internal stresses owing to the constraint imposed by the metallic conductor. Previous studies have demonstrated that sub-T_g thermal annealing can induce local segmental relaxation and rearrangement of the amorphous structure, leading to changes in the free volume and redistribution of residual stresses.[19] As shown in Fig. 6(f), 130 °C alone may be insufficient to induce significant macroscopic mechanical changes in freestanding TPI films. However, on the outer arc of the circular coil (bending radius of 3 cm), where the bending strain approaches the local cracking threshold, even a minor degree of structural relaxation and stress redistribution may be sufficient to trigger microcrack initiation.

Such sub-T_g structural relaxation also directly accounts for the observable differences in the appearance of the wires before and after thermal treatment. As shown in Fig. 7(a), the photograph presents a comparison between the original TPI-1 wire and the cracked TPI-2 wire cut from the prototype. When observed at the same length, the TPI-1 wire showed a naturally bent state, whereas the TPI-2 wire retained a coil-like bent shape, exhibiting an irreversible heat-setting phenomenon. In addition, it was found that the TPI insulation layer of the TPI-1 could be pulled off the conductor relatively easily during wire stripping operation. In contrast, for a cracked wire, the TPI insulation layer cannot be pulled off even if the metal conductor is broken. This result indicates that heat treatment during the VPI process exerted an irreversible effect on the TPI material itself.

As shown in Fig. 7(b), the coefficient of thermal expansion (CTE) of the TPI film was determined to be 6.725×10^{-5}/°C, while that of the TPI tube was 5.052×10^{-5}/°C. These values were considerably higher than those of the metal conductor (approximately 1.7×10^{-5}/°C). This mismatch indicates that the insulation layer underwent thermal deformation during the VPI process, thereby generating substantial thermal stress.[20] However, the temperature during the VPI process is only 130 °C, far below the T_g of TPI. For ideal stress-free polymer systems, thermally induced dimensional changes below T_g are generally reversible elastic responses unless the resulting thermal stress exceeds the yield strength of the material. Therefore, sub-T_g segmental relaxation, as evidenced previously, can lead to irreversible structural rearrangement and internal stress redistribution, which are critical factors in the observed behavior. This structural evolution leads to a secondary setting of the insulation layer during thermal treatment, resulting in the insulation firmly gripping the conductor.

The SEM fracture morphologies revealed that different treatment conditions exerted a pronounced influence on the fracture behavior of the TPI insulation layer. The fracture surface of the pristine TPI-1 wire in Fig. 8(a) exhibits a relatively high overall roughness, with prominent radial tear ridges, fibrillated and stretched deformation zones, and relatively locally flat regions. This morphology indicates that pristine TPI possesses a certain capacity for plastic deformation and energy dissipation during fracture. The directional nature of tear patterns may also be associated with the molecular chain orientation and frozen-in residual stresses introduced during the wire extrusion process. After thermal treatment at 130 °C for 3 days (Fig. 8b), the fracture surface becomes generally flatter. The pronounced radial fibrillation and deep tearing features observed in the pristine sample were markedly reduced, and were replaced by relatively shallow lamellar- or river-like tear patterns and localized slip marks. This suggests that the extent of large-scale plastic deformation during fracture is diminished after thermal treatment, and that crack propagation tends to proceed along more localized, concentrated pathways. Considering that the T_g, T_m, and macroscopic mechanical properties remain essentially unchanged, the XRD results confirm a persistent amorphous state, and that the cold crystallization temperature decreases while the cooling

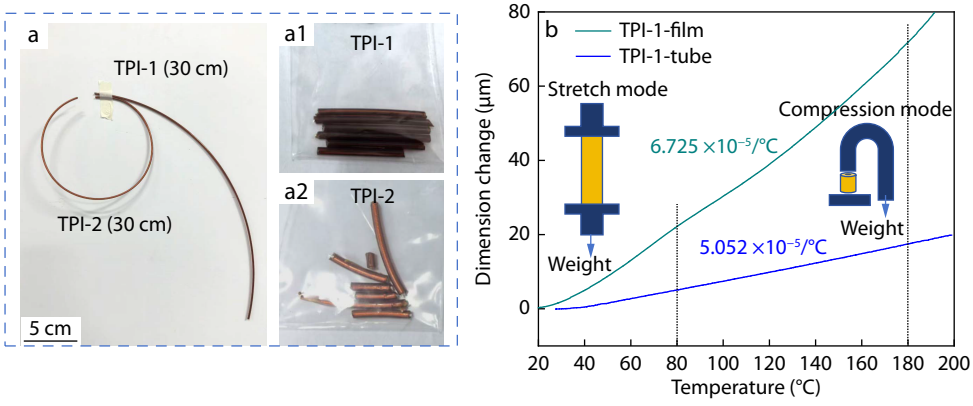


Fig. 7 (a) Photograph of the pristine wire (TPI-1) and the cracked wire (TPI-2) of the same length; (a1, a2) The corresponding TPI insulation tubes after removal of the metallic conductor; (b) Thermal expansion curves of the TPI-1 film and the TPI-1 tube.

https://doi.org/10.1007/s10118-026-3878-0

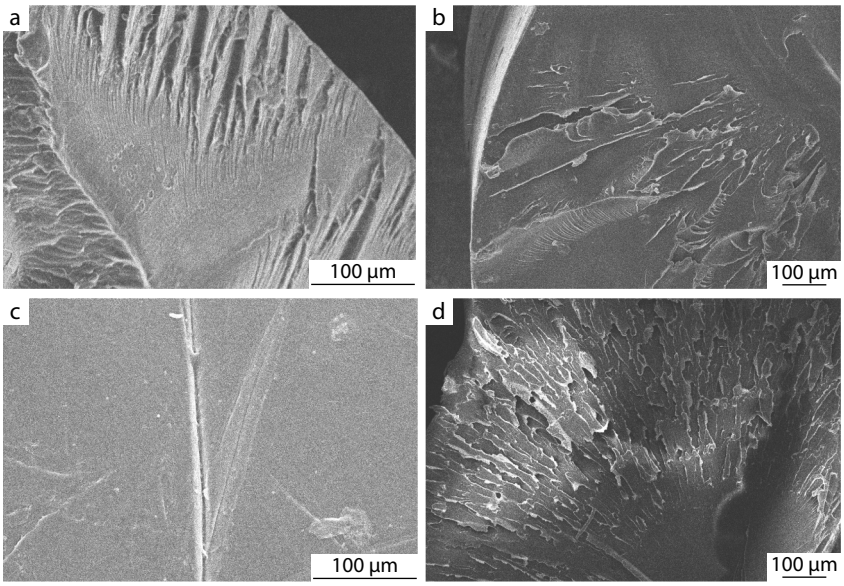


Fig. 8 SEM images of the wire insulation layer. (a) The cross-section of TPI-1, (b) the cross-section of TPI-2, (c) surface cracks on TPI-2, (d) the cross-section of TPI-1 coated with epoxy resin mixture.

crystallization temperature increases. We are more inclined to attribute the observed changes to sub-T_g structural relaxation and local rearrangement of chain segments rather than to crystallization or main-chain thermal degradation. Such relaxation leads to alterations in the free volume, molecular packing, and redistribution of extrusion induced residual stresses, thereby modifying local resistance to crack initiation. In Fig. 8(c), a narrow and continuous surface crack is observed, with no significant voids or melting-induced damage on either side of the crack, suggesting that the crack most likely initiated from surface defects or stress concentration sites on the outer arc under sustained tensile stress and then propagated inward. In contrast, the sample after surface contact with the epoxy resin (Fig. 8d) exhibits a fracture morphology distinctly different from that of the thermally treated sample, characterized by extensive and dense radial tear ridges, fibrillated structures, and localized pull-out features. This morphology indicates a more intense and heterogeneous local deformation prior to fracture. These features are consistent with the permeation of low molecular weight components from the epoxy system into the amorphous regions of the TPI, which induced localized swelling, reduced interchain interactions, and enhanced segmental mobility. As a result, the insulation layer becomes more susceptible to localized yielding, microvoiding, and crack initiation under the applied bending stress. Overall, the SEM results support two distinct but superimposable failure mechanisms: prolonged thermal treatment at 130 °C promotes cracking in the bent region primarily through sub-T_g structural relaxation, residual stress redistribution, and localized reduction in crack resistance; while contact with the curing agent further accelerates failure by enhancing ESC susceptibility through low-molecular-weight permeation, plasticization, and swelling effects.

In summary, the failure of TPI-insulated wires during VPI processing is attributed to the complex interplay of thermal, mechanical, and chemical factors. Mechanistically, the bent geometry imposes a sustained tensile stress on the outer arc of the insulation layer, whereas, the extrusion process imparts molecular orientation and residual stresses that are frozen into the TPI matrix during rapid cooling. Despite the fact that the ageing temperature (130 °C, 72 h) is far below the T_g, it is nonetheless sufficient to induce sub-T_g structural relaxation and amorphous phase reorganization, accompanied by measurable changes in free volume and residual stress distribution. The constraining effect of the metallic conductor further inhibits the dimensional recovery of the insulation, ultimately driving the highly strained outer arc toward the critical state for microcrack initiation. Concurrently, low-molecular-weight penetrants—notably HY918 and DY073-1—migrate into the amorphous domains of TPI, where they promote plasticization, localized swelling, and enhanced segmental dynamics, thereby compromising the local yield strength and fracture toughness. Under the combined influence of sustained bending tensile stress, thermal expansion mismatch and penetrant-induced degradation, a classical ESC mechanism is established, which significantly accelerates the overall failure process.

Verification of Protection Schemes

From the aforementioned analysis, it can be concluded that both the plasticization effect of the epoxy resin mixture and prolonged heat treatment can induce structural transformations in the TPI materials, which in turn leads to cracking at the bent parts. Therefore, an optimized protection scheme was designed in this study, as shown in Fig. 9(a). Specifically, an aerogel thermal insulation film based on a polyimide substrate was spirally wrapped around the TPI wires of the prototype. To verify the thermal insulation effect of the insulation film, a thermocouple was first attached to the wire surface, as shown in Fig. 9(b). The insulation film was then wrapped around the thermocouple, and hot air was blown onto the wrapped region using a hot air gun, as shown in Fig. 9(c). The protection method for the sample extension leads is shown in Fig. 9(e): the insulation film was first wrapped around the surface of the sample lead wires, and the excess wires were then coiled into a circular shape to facilitate VPI operation (Fig. 9f). The Paschen test setup is shown in

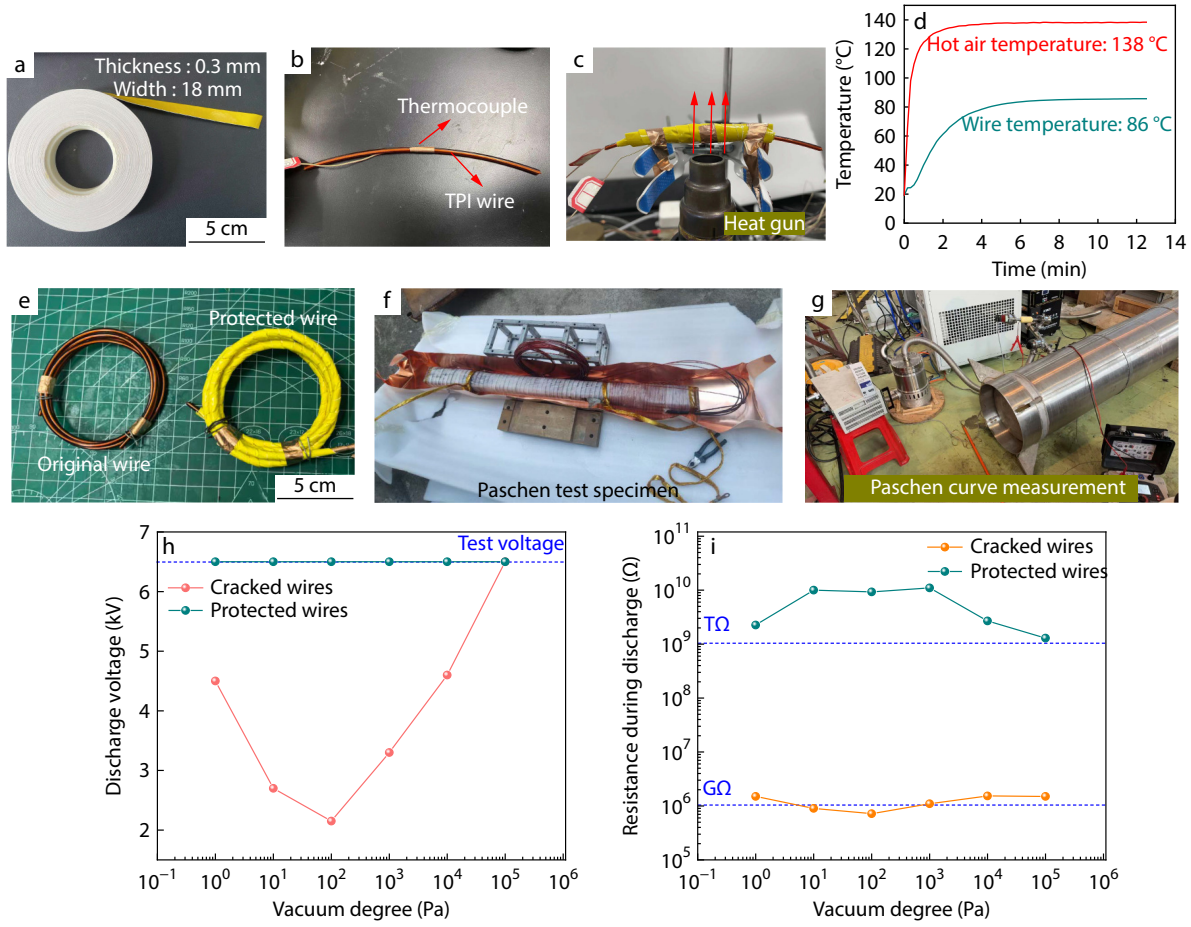


Fig. 9 (a) Photograph of the thermal insulation film; (b, c) Photographs of the thermal protection test on TPI wires wrapped with thermal insulation film; (d) Curves of cable surface temperature and hot air temperature versus time; (e) Photographs of the original TPI coil and the TPI coil with thermal insulation protection; (f) VPI test specimen; (g) Paschen test setup, including a vacuum chamber, a vacuum pump and an insulation resistance tester; (h) Curves of discharge voltage versus vacuum degree for the cracked wire and the protected wire in the Paschen test; (i) Curves of insulation resistance versus vacuum degree at discharge voltage.

Fig. 9(g): the stainless steel armor inside the sample was connected to the positive terminal of the power supply, and the insulating material surface was connected to the negative terminal. The sample was placed in a vacuum chamber to measure the discharge voltage and resistance values at different vacuum levels. Subsequently, the VPI treatment was performed in accordance with the scheme illustrated in Fig. 1(e). Finally, the prototype was removed for the Paschen testing.The thermal insulation film serves two key functions: on one hand, it provides physical protection to block epoxy resin contamination; on the other hand, it prevents heat penetration, thereby reducing the coil surface temperature and inhibiting the relaxation behavior of TPI. The results of the thermal insulation tests are shown in Fig. 9(d). After wrapping with the thermal insulation film (thickness: 0.3 mm, overlap rate: 50%), the wire surface temperature can be reduced to below 86 °C. The Paschen test results are shown in Figs. 9(h) and 9(i). For the prototype with cracked TPI wires, the discharge voltage under different vacuum degrees was lower than the preset 6.5 kV, and the insulation resistance decreased to the GΩ level. This fails to meet the standard requirement of a leakage current below 20 μA in the 6.5 kV Paschen test. In contrast, the stainless-steel armored prototype welded with TPI wires protected by the thermal insulation film achieved a preset discharge voltage under various vacuum degrees, demonstrating that the diagnostic wire still maintains excellent insulation performance.

CONCLUSIONS

The present work provides a comprehensive investigation of the cracking failure of TPI-insulated wires encountered during the VPI process. The experimental evidence unequivocally demonstrates that the observed cracking is not attributable to a single cause but rather arises from a complex interplay of thermal, mechanical, and chemical degradation mechanisms. The geometrical constraint of the coiled configuration subjects the outer arc of the insulation to a sustained bending tensile stress, whereas the wire extrusion process introduces frozen-in molecular orientation and residual stresses within the TPI layer. Heat treatment induces sub-T_g segmental relaxation and local rearrangement of the amorphous structure, resulting in alterations in the free volume and redistribution of residual stresses, ultimately promoting microcrack initiation at the highly strained outer arc. The migration of HY918 and DY073-1 into TPI caused plasticization, localized swelling, and enhanced chain segmental mobility, which collectively reduced the local yield strength

https://doi.org/10.1007/s10118-026-3878-0

and fracture resistance. The significant mismatch in the CTE between the TPI insulation and metallic conductor generates substantial thermal stresses during the VPI thermal cycle, further amplifying the driving force for crack propagation. Based on these mechanistic insights, a protective countermeasure was developed to prevent cracking during the VPI process. Thermal insulation wrap was employed both as a barrier against epoxy resin contact and as a buffer against the thermal exposure. This study provides new insights into improving the weatherability and insulation reliability of TPI wires in practical applications.

Conflict of Interests

The authors declare no interest conflict.

Electronic Supplementary Information

Electronic supplementary information (ESI) is available free of charge in the online version of this article at http://doi.org/10.1007/s10118-026-3878-0.

Data Availability Statement

The data related to this paper are data that should not be shared. The data can be obtained from the author for reasonable reasons. Author's contact information: Chao Xiao, e-mail: cxiao@issp.ac.cn.

ACKNOWLEDGMENTS

This work was financially supported by the Comprehensive Research Facility for Fusion Technology Program of China (No. 2018-000052-73-01-001228), Research on Performance Improvement and Key Technology of Quench Detection System of EAST Device of China (No. E05F0K153Z1), and the National Natural Science Foundation of China (No. 52403120).

REFERENCES

1 Wu, G.; Qi S.; Tian G.; Wu D. Preparation and characterization of low cte thermoplastic copolyimide resins based on the structural design of block sequence. *Eur. Polym. J.* **2023**, *195*, 112249.
2 Cao, X.; Yang S.; Huang Q.; Pan Z.; Xie Y.; Tong Y.; He K.

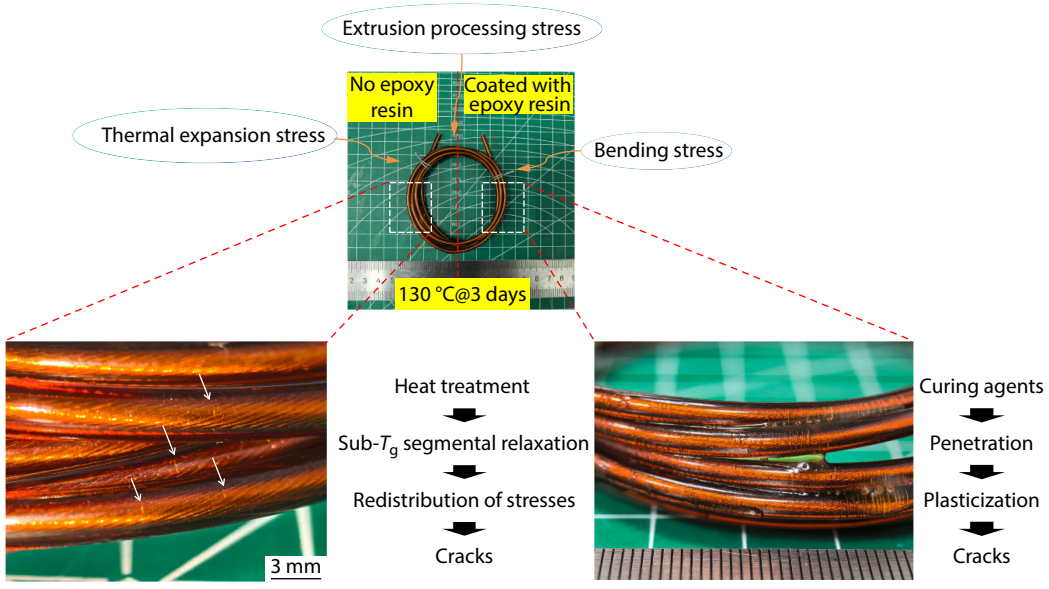
Graphical Abstract

Cracking Behavior Analysis of Thermoplastic Polyimide under Vacuum Pressure Impregnation

Chao Xiao, Xian Zhang, Long-Gui Zheng, Ye-Zheng Xiao, and Yan-Lan Hu

Hefei Institutes of Physical Science, Chinese Academy of Sciences

Thermoplastic polyimide (TPI) wire failure during vacuum pressure impregnation (VPI) is caused by sub-T_g relaxation under bending/thermal stress and environmental stress cracking (ESC) from epoxy penetrants. A thermal insulation wrap effectively blocked resin permeation and thermal damage, as confirmed by the vacuum Paschen test.



Chinese J. Polym. Sci. 2026 *https://doi.org/10.1007/s10118-026-3878-0*

Thermoplastic polyimides with enhanced processability and thermal stability *via* molecular structure modulation. *Polym. Eng. Sci.* **2025**, *65*, 5389–5401.
3 Hall, M. A.; Lewis, B.; Shull, K. R. Thermomechanical characterization of high Tg disulfide-containing thermoplastic polyimides. *Macromolecules* **2025**, *58*, 2065–2072.
4 Nazarychev, V. M.; Pavlov, A. A.; Kamalov, A. M.; Borisova, M. E.; Didenko, A. L.; Ivan'kova, E. M.; Kraft, V. E.; Vaganov, G. V.; Nikolaeva, A. L.; Ivanova, A. S.; Lavrentiev, V. K.; Popova, E. N.; Abalov, I. V.; Blokhin, A. N.; Bugrov, A. N.; Kudryavtsev, V. V. The effect of synthesis conditions and chemical structure of thermoplastic polyimides on their thermomechanical properties and short-term electrical strength. *Polymers* **2025**, *17*, 1385.
5 Gao, J.; Auchmann, B.; Hug, C.; Pautz, A.; Sanfilippo, S. Study of a current-based quench detection method for cct magnets *via* a co-wound superconducting sensing wire. *IEEE Trans. Appl. Supercond.* **2021**, *31*, 4701105.
6 Miyoshi, Y.; Bruton, A.; Cormany, C.; Liao, M.; Mitchell, N.; Schild, T.; Barden, R.; Everitt, D.; Freudenberg, K.; Guilliams, V.; Hughes, D.; Martovetsky, N.; Rossano, G.; Vandergriff, D.; Wooley, K.; Khumthong, K.; Norausky, N.; Ortiz, E.; Sheeron, J.; Smith, J. Selected topics of technical challenges of the ITER central solenoid. *IEEE Trans. Appl. Supercond.* **2024**, *34*, 4205405.
7 Piccin, R.; Rigaud, J. S.; Santillana, I. A.; Buchanan, K. E.; Ternova, D.; Mitchell, N.; Liao, M.; Luongo, C. Environmental stress cracking of thermoplastic polyimide insulated wires. *IEEE Trans. Appl. Supercond.* **2024**, *34*, 7700405.
8 Goodwin, A. A.; Whittaker, A. K.; Jack, K. S.; Hay, J. N.; Forsythe, J. Absorption of low molecular weight penetrants by a thermoplastic polyimide. *Polymer* **2000**, *41*, 7263–7271.
9 Clayton, N.; Evans, D.; Gung, C. Y.; Pastor, O.; Piccin, R.; Cerignat, S.; Huang, X.; Li, G.; Crouchen, M. Extraction of instrumentation wires through the high-voltage insulation of the ITER magnet feeder system. *IOP Conf. Ser. Mater. Sci. Eng.* **2019**, *502*, 012185.
10 Rudeiros Fernández, J. L.; Navarro, C.; Arbelaez, D.; Ferracin, P.; Prestemon, S.; Shen, T.; Vallone, G. Interface characterization for superconducting magnets. *IEEE Trans. Appl. Supercond.* **2024**, *34*, 4703105.
11 Hsieh, A. J.; Desper, C. R.; Schneider, N. S. Transient crystallization of an aromatic polyetherimide: effect of annealing. *Polymer* **1992**, *33*, 306–313.
12 Sung Chun, Y.; Weiss, R. A. Thermal behavior of poly(ether ketone ketone)/thermoplastic polyimide blends. *J. Appl. Polym. Sci.* **2004**, *94*, 1227–1235.
13 Zi, Y. C.; Wu, G. J.; Pei, D. X.; Guo, S.; Qi, S. L.; Tian, G. F.; Wu, D. Z. Decreasing the CTE of thermoplastic polyimide by blending with a thermosetting system. *Chinese J. Polym. Sci.* **2023**, *41*, 956–961.
14 Huo, P. P.; Friler, J. B.; Cebe, P. NEW-TPI thermoplastic polyimide: thermal analysis and small-angle X-ray scattering. *Polymer* **1993**, *34*, 4387–4398.
15 Hsiao, B. S.; Sauer, B. B.; Biswas, A. Crystallization study of a thermoplastic polyimide (new-TPI). *J. Polym. Sci. Part B Polym. Phys.* **1994**, *32*, 737–747.
16 He, J.; Niu, X.; Chen, W.; Chen, W.; Yu, Y.; Fan, H. Preparation and properties of soluble thermoplastic polyimides with phenol side-groups for flexible copper clad laminates. *High Perform. Polym.* **2025**, *37*, 271–285.
17 Robertson, C. G.; Monat, J. E.; Wilkes, G. L. Physical aging of an amorphous polyimide: enthalpy relaxation and mechanical property changes. *J. Polym. Sci. B Polym. Phys.* **1999**, *37*, 1931–1946.
18 Arnold, F. E. Jr, Bruno, K. R.; Shen, D.; Eashoo, M.; Lee, C. J.; Harris, F. W.; Cheng, S. Z. D. The origin of β relaxations in segmented rigid-rod polyimide and copolyimide films. *Polym. Eng. Sci.* **1993**, *33*, 1373–1380.
19 Ree, M.; Swanson, S.; Volksen, W. Effect of precursor history on residual stress and relaxation behaviour of high temperature polyimides. *Polymer* **1993**, *34*, 1423–1430.
20 Gautreaux, C. R.; Pratt, J. R.; St Clair, T. L. A study of crystalline transitions in a thermoplastic polyimide. *J. Polym. Sci. Part B Polym. Phys.* **1992**, *30*, 71–82.

https://doi.org/10.1007/s10118-026-3878-0